Mon. Not. R. Astron. Soc. **000**, 000–000 (0000) Printed 12 September 2012 (MN LATEX style file v2.2)

A new L-dwarf member of the moderately metal-poor triple system HD 221356

B. Gauza[1,2] ⋆, V. J. S. Béjar[1,2], R. Rebolo[1,2,3], K. Peña Ramírez[1,2], M. R. Zapatero Osorio[4], A. Pérez-Garrido[5], N. Lodieu[1,2], D. J. Pinfield[6], R. G. McMahon[7,8], E. González-Solares[7], J. P. Emerson[9], S. Boudreault[1,2], M. Banerji[7]

[1]*Instituto de Astrofísica de Canarias (IAC), E-38200 La Laguna, Tenerife, Spain*
[2]*Dept. Astrofísica, Universidad de La Laguna (ULL), E-38206 La Laguna, Tenerife, Spain*
[3]*Consejo Superior de Investigaciones Científicas, Madrid, Spain*
[4]*Centro de Astrobiología (CSIC-INTA), E-28850 Torrejón de Ardoz, Madrid, Spain*
[5]*Universidad Politécnica de Cartagena, Campus Muralla del Mar, Cartagena, Murcia E-30202, Spain*
[6]*Centre for Astrophysics Research, Science and Technology Research Institute, University of Hertfordshire, Hatfield AL10 9AB*
[7]*Institute of Astronomy, University of Cambridge, Madingley Road, Cambridge CB3 0HA, UK*
[8]*Kavli Institute for Cosmology, University of Cambridge, Madingley Road, Cambridge CB3 0HA, UK*
[9]*Astronomy Unit, School of Physics & Astronomy, Queen Mary University of London, London, E1 4NS, UK.*

12 September 2012

ABSTRACT

We report on the discovery of a fourth component in the HD 221356 star system, previously known to be formed by an F8V, slightly metal-poor primary ($[\mathrm{Fe/H}] = -0.26$), and a distant M8V + L3V pair. In our ongoing common proper motion search based on VISTA Hemisphere Survey (VHS) and 2MASS catalogues, we have detected a faint $J = 13.76 \pm 0.04$ mag) comoving companion of the F8 star located at angular separation of 12.13 ± 0.18 arcsec (position angle of 221.8 ± 1.7 deg), corresponding to a projected distance of $\sim$312 au at 26 pc. Near-infrared spectroscopy of the new companion, covering the 1.5–2.4 micron wavelength range with a resolving power of R$\sim$600, indicates an L1$\pm$1 spectral type. Using evolutionary models the mass of the new companion is estimated at $\sim$0.08 solar masses, which places the object close to the stellar-substellar borderline. This multiple system provides an interesting example of objects with masses slightly above and below the hydrogen burning mass limit. The low mass companions of HD 221356 have slightly bluer colours than field dwarfs with similar spectral type, which is likely a consequence of the sub-solar metallicity of the system.

Key words: stars—low-mass, brown dwarfs—stars—individual: HD 221356

1 INTRODUCTION

Because of progressive cooling with age, brown dwarfs do not obey a unique mass-luminosity relation (Burrows et al. 1997, 2001). Therefore, the determination of a brown dwarf mass requires either a good knowledge of its age or a direct dynamical measurement. This, in turn, is possible for substellar companions of stars or for those that are found in multiple systems. An additional advantage is that the metallicity can be inferred from the primary star. For solar-type stars the atmospheres are much better understood than for very low-mass stars and brown dwarfs, given the poor knowledge of opacities in cool atmospheres (Bean et al. 2006; Bonfils et al. 2005). Coeval systems containing low-mass companions also provide very useful constraints on evolutionary and atmospheric models (e.g. Pinfield et al. 2006; Dupuy et al. 2010) as well as offering a rather unique view on how the process of star formation works at the very bottom of the main sequence (Burgasser et al. 2007). In particular, brown dwarf companions with well determined metallicities are benchmark objects allowing for a better understanding of the effects of metallicity on the physical properties and evolution of substellar objects (Pinfield & et al. 2012). Unfortunately, substellar companions located at wide separations (>50 au) from their parent stars are relatively rare, with an estimated frequency of less than a few per cent (McCarthy & Zuckerman 2004; Lafrenière & et al. 2007; Kraus & Hillenbrand 2007).

We are conducting a search for very low-mass common proper motion companions of nearby ($\lesssim$ 25 pc) stars, using the VISTA Hemisphere Survey (VHS) (McMahon et al., in preparation) and Two Micron All Sky Survey (2MASS) (Skrutskie & et al. 2006). Our sample of objects includes some of the known multiple sys-

⋆ e-mail:bgauza@iac.es

Table 1. Properties of HD 221356A (a.k.a. HR 8931, HIP 116106).

Parameter	Value	References
RA. (J2000)	$23^{\rm h}31^{\rm m}31\overset{\rm s}{.}62$	-
Dec. (J2000)	$-04°05'16\overset{''}{.}78$	-
V (mag)	6.50	1
Spectral type	F8.0 V	3
$\mu_\alpha \cos(\delta)$	178.7 ± 0.9 mas/yr	2
μ_δ	-192.8 ± 0.9 mas/yr	2
Parallax	38.29 ± 0.54 mas	2
Distance	26.12 ± 0.37 pc	2
$T_{\rm eff}$	5976 ± 44 K	1
$\log(g)$	4.31 ± 0.06 cm/s^2	1
Mass	0.94 ± 0.13 M$_\odot$	1
[Fe/H]	-0.26 ± 0.03	1
Age	$2.5 - 7.9$ Gyr	1
1) Valenti & Fischer (2005)	2) van Leeuwen (2007)	
3) Caballero (2007)		

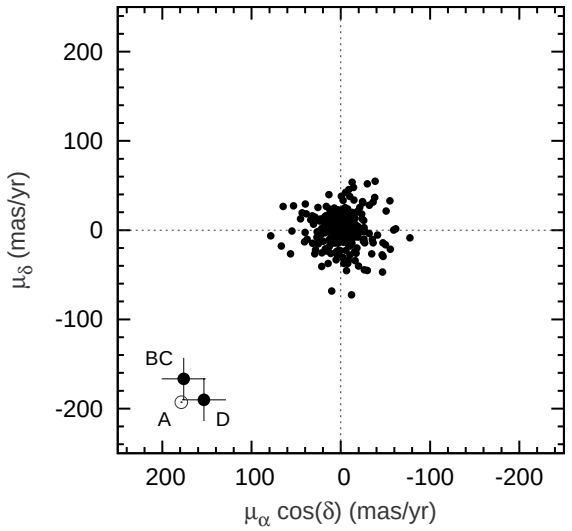

Figure 1. Proper motion vector-point diagram for the HD 221356 system. All correlated objects within 15 arcmin from the primary are plotted as black dots, with HD 221356 components labelled as A, BC and D. The primary is saturated in both surveys, its proper motion value was taken from the literature. Time baseline between the 2MASS and VHS epochs is 12.18 years.

tems (Faherty et al. 2010 and references therein). One of the targets investigated so far was HD 221356, already known to be a triple system. The F8.0 V primary is a field star with slightly subsolar metallicity $[{\rm Fe/H}] = -0.26$ (Valenti & Fischer 2005), located at 26.12 ± 0.37 pc (van Leeuwen 2007). The main properties of this star are given in Table 1. Gizis et al. (2000) reported that the secondary, initially described as a single object, has a photometric distance consistent with that of the HD 221356 star determined by *Hipparcos*. The secondary was later resolved by Close et al. (2002) into a binary separated by 0.57 arcsec (∼14.9 au), using adaptive optics on the Gemini North Telescope. Based on their photometric colours, they estimated spectral types of M8.0 V and L3.0 V for each of the two components, respectively. This binary (hereafter referred to as HD 221356BC) was also investigated by Caballero (2007). Using data at epochs separated by 48.3 years, he confirmed a common proper motion between HD 221356A and BC. He also measured a mean separation of $\rho = 451\overset{''}{.}8 \pm 0\overset{''}{.}4$ between both components, which corresponds to a projected physical separation of nearly twelve thousand au, making it one of the widest known systems with an L-type component (see also fig 11 of Zhang & et al. 2010).

In this article we present the identification and characterization of a fourth, very low-mass companion of the HD 221356 system. We outline the procedure and results of our proper motion search together with the analysis of I and $YJHK_s$-band photometry and near-infrared spectroscopic data of the identified companion. We derive the physical properties of the new object which turns out to be very close to the hydrogen burning mass limit.

2 IDENTIFICATION AND FOLLOW-UP OBSERVATIONS

2.1 VISTA Hemisphere Survey data

The new low-mass companion of HD 221356 A was identified using the 2MASS and VHS catalogues. The VHS is a near-infrared public survey intended to cover the entire Southern hemisphere ($\sim 20,000$ deg^2) in the JK_s broad band filters with a sensitivity more than 3 mag deeper than 2MASS. It uses the 4.1-m telescope VISTA (Visible and Infrared Survey Telescope for Astronomy) operating since 2009 at ESO's Cerro Paranal Observatory in Chile (Emerson et al. 2006). It is equipped with a wide-field near-infrared camera (VIRCAM), comprising sixteen 2k×2k pixel detectors with a mean plate scale of 0.339 arcsec. The HD 221356 system was observed with VISTA on 2010 November 25 and 26. Average seeing conditions were $1.4''$ and $0.9''$, respectively.

The VHS near-infrared images are processed and calibrated automatically by a dedicated science pipeline implemented by the Cambridge Astronomical Survey Unit (CASU). Standard reduction and processing steps include dark and flat-field corrections, sky background subtraction, linearity correction, destripe and jitter stacking. For more detailed description we refer to the CASU webpage http://casu.ast.cam.ac.uk/surveys-projects/vista, as well as to Irwin & et al. (2004) and Lewis et al. (2010).

2.2 Proper motion

The search for additional common proper motion companions of HD 221356 A was done using the astrometry given in the VHS and 2MASS catalogues, which provide a 12.18 yr baseline. The positions of 2MASS sources have an estimated accuracy of 70-80 mas over the magnitude range of $9 < K_s \leq 16$ (Skrutskie & et al. 2006). The astrometric solution for VHS observations is done automatically as part of the CASU pipeline, using the 2MASS point source catalogue. The objects on the catalogues extracted from each VISTA detector are matched to their counterparts in 2MASS using a correlation radius of 1 arcsec. Because 2MASS has a high degree of internal consistency it is possible to calibrate the world coordinate system of VISTA images to better than 0.1 arcsecond.

The search was performed using TOPCAT,[1] a useful tool for analysis and manipulation of source catalogues and other data tables, developed as part of the Virtual Observatory. We retrieved the

[1] http://www.star.bris.ac.uk/∼mbt/topcat/

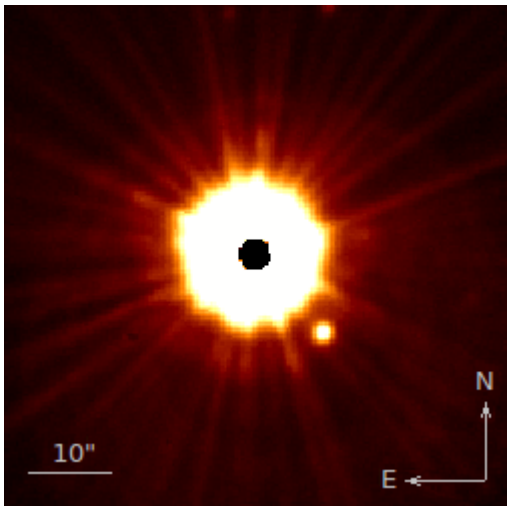

Figure 2. False colour VISTA *J*-band image of HD 221356AD. Angular separation is 12.13 ± 0.18 arcsec and the position angle of the identified companion is 221.8 ± 1.7 degrees. Saturation in the centre of the primary is visible. Field-of-view is 1×1 arcmin, with North up and East to the left.

astrometric and photomeric data from both 2MASS and VHS catalogues, for all the objects within a radius of 15 arcmin corresponding to ∼23,000 au around the examined star. To avoid some of the spurious detections, we selected sources brighter than J=17 mag in 2MASS. We have cross-matched 300 objects from both catalogues within 1 arcsec. The sources that remained unmatched were subsequently cross correlated taking into account the proper motion of the primary star provided by *Hipparcos* (van Leeuwen 2007). We illustrate the resulting proper motion vector-point diagram of HD 221356 on Figure 1.

We have found that the proper motion of HD 221356 BC (Table 2) is consistent with that of the primary HD 221356 A, thereby confirming the result of the Königstuhl survey of Caballero (2007). Individual components of the BC pair, separated by only 0.57 arcsec (Close et al. 2002), were not resolved in the VHS images. We also identified a new common proper motion companion (2MASS J23313095-0405234, hereafter HD 221356 D), with $(\mu_\alpha \cos\delta,\ \mu_\delta) = (153.48 \pm 21, -190.20 \pm 19)$ mas/yr, located 12.13 ± 0.18 arcsec southwest from the primary. We adopted a total astrometric uncertainty of ~ 28 mas/yr, estimated using the standard deviation of proper motions for sources with $\mu < 100$ mas/yr. The proper motion of the new object is common with that of the HD 221356 system. Measured separations, position angles and proper motions are listed in Table 2.

2.3 Photometry

The VHS catalogue provides aperture photometry for HD 221356 in the $YJHK_s$ near-infrared bands. The VISTA photometric system is calibrated using the magnitudes of colour selected 2MASS stars converted onto the VISTA system using colour equations, including terms to account for interstellar reddening[2]. Photometric calibrations are determined to an accuracy of 1-2%.

The new faint companion HD 221356 D is well resolved in the VHS images (see Figure 2), but within the glare of the primary. In order to minimize the possible light contamination in the aperture photometry of the VHS catalogue, we applied a method to suppress the PSF of the primary by subtracting the flipped and rotated images from the original ones. Standard deviation of the background at the same separation as the companion was a factor two lower in the PSF subtracted images than in the original ones, which slightly improves the detection of the object. We performed aperture photometry on the resultant images with an aperture of one full-width half-maximum (FWHM). The instrumental magnitudes were then calibrated to apparent magnitudes by adding the aperture corrections determined using the VHS photometry of fourteen isolated bright stars located within 10 arcmin from HD 221356A. The differences between the new and the catalogue photometry in the Y, J, H and K_s bands are 0.53 ± 0.06, 0.26 ± 0.04, 0.15 ± 0.03, 0.13 ± 0.03 mag, respectively. Photometric values for the BC companion were taken directly from the VHS source catalogue.

Table 2. Proper motion, separations and position angles of low mass components of the HD 221356 system.

Comp.	$\mu_\alpha \cos(\delta)$ (mas/yr)	μ_δ (mas/yr)	ρ* (arcsec)	θ* (deg)	r (au)
BC	176 ± 21	-167 ± 19	451.10 ± 0.18	261.77 ± 0.04	11900 ± 50
D	154 ± 21	-190 ± 19	12.13 ± 0.18	221.8 ± 1.7	317 ± 9

* epoch (MJD) = 55525.12460836; ρ, θ and r are measured with respect to the primary.

On November 15th, 2011 we performed follow-up I-band imaging of HD 221356 AD. Observations were carried out using the IAC80 telescope equipped with a E2V 2048×2048 back illuminated CCD detector with a plate scale of 0.304 arcsec/pix, which provides a 10.4×10.4 arcmin field of view. We selected the 12 images with best seeing (FWHM$<$1.2 arcsec) to minimize interference from the primary star. We reduced the images applying standard techniques, including bias and flat-field correction, using IRAF routines. Individual exposure times were 5s. For each image, we performed a similar method for the PSF subtraction of the primary as used for VISTA images and subsequently aligned and combined all of them. We obtained the PSF-fit photometry using the DAOPHOT package in IRAF and calibrated the instrumental magnitude of our object using 11 bright stars in the field with DENIS (Epchtein & et al. 1999) I-band data available. We note that the photometric system used (Cousin) is not the same as the one of DENIS, and that some differences may appear for very cool objects, however in our previous photometric calibrations we found that the zeropoint between IAC80 and Denis I-band has small colour dependence (Costado et al. 2005).

Additionally, we acquired I-band observations of HD 221356 A using FastCam, mounted on the 1.5-m Carlos Sánchez Telescope at the Teide Observatory on January 31, 2012. FastCam is a lucky imaging instrument, designed to perform high spatial and time resolution observations (Oscoz & et al. 2008). Optics provide a plate scale of 43.5 mas/pix, and a field of view of $\sim 22 \times 22$ arcsec^2. We obtained 17 blocks of 1000 images of 50 ms individual exposure times. Images were bias corrected, aligned and stacked into the final image using the software provided by the FastCam team. We derived the I-band aperture photometry of the primary, since we found that the literature values based on photographic plates are not reliable. Instrumental magnitudes were calibrated using photometric standard stars from Landolt (1992) observed at different airmasses along the night under photometric conditions. We also explored the inner region to search for the

[2] http://casu.ast.cam.ac.uk/surveys-projects/vista/technical/photometric-properties

presence of additional companions, but none were identified. We may exclude the presence of an equal mass companion to the primary at separations greater than 0.2″ (∼5 au) and companions with $\Delta I < 5$ mag at separations greater than 1″ (∼26 au).

The photometric data are listed in Table 3. The *I*-band magnitudes of the distant BC pair were taken from Gizis et al. (2003) who imaged individual components with Hubble Space Telescope WFPC2. The integrated JHK_s photometry of the BC component from VHS were also decomposed into individual magnitudes using the flux ratios derived by Close et al. (2002). The JHK_s band photometry of the primary, also given in Table 3, is from the 2MASS catalogue.

2.4 Near-IR spectroscopy

We also obtained near-infrared spectroscopy of the HD 221356 AD system and the M8V spectroscopic standard LP 412-31 (Kirkpatrick et al. 1995) using LIRIS, with the *HK* grism and the 1K×1K Hawaii detector at the 4.2 m William Herschel Telescope (WHT) on December 30 2011. This instrumental configuration provides a nominal dispersion of 9.7 Å pix^{-1} and a wavelength coverage of 1.4–2.4 μm. A slit width of 0.75" was used rotated to the direction along the AD system and the final resolution of the spectrum was 26 Å(R ∼ 600). Total integration time was 2240 s, divided into individual exposures of 160s. A nodding pattern of two positions (AB) was used to subtract the sky background. Weather conditions were photometric and the average seeing was 0.9". Data were dark corrected, sky subtracted, aligned and combined at each nodding position. Flat-field correction using a tungsten lamp was not applied due to a spurious feature in the *K*-band tungsten spectrum. After subtracting the contribution of the primary wings, spectra of HD 221356 D were optimally extracted using the APALL routine and wavelength calibrated using ArXe arc lines. We finally combined the spectra at both AB positions and corrected for telluric absorption lines by dividing them by the A3V star HR8840, observed at a similar airmass, and multiplying by a blackbody of the corresponding effective temperature of 8500 K. Spectroscopic data of LP 412-31 were reduced and analized in a similar way to HD 221356 D, but telluric correction was done using the A3V star HR 1036, also observed at a similar airmass. Spectra of HD 221356 D and LP 412-31 in comparison with other standard objects and the main spectroscopic features are shown in Figure 3.

HD 221356 D displays stronger water vapor absorption bands than the standard M8 dwarf observed with the same instrumental setup and sky conditions and reduced in the same manner as our target. This implies that HD 221356 D has a cooler spectral type, quite likely within the L domain. Aimed at deriving the spectral type of HD 221356D, we have compared its LIRIS spectrum with data extracted from the IRTF libraries (Cushing et al. 2005), see Fig. 3. We note that these data correspond mostly to dwarfs with solar composition. The overall *HK* spectral energy distribution (SED) of HD 221356D is better reproduced by a spectral type of L0-L1. However we determine a spectral type of L1–L3 if we consider the different water indexes at ∼ 1.7 or 2.0 μm (Testi & et al. 2001; Allers & et al. 2007; Slesnick et al. 2004). The differences can be explained if the object is slightly metal poor (consistent with the primary), because the *K*-band flux should be reduced by the H_2 collisional induced absorption. The strength of the sodium feature at 2.2 microns in object D compares better with solar metallicity M9 dwarf than with the early L-type templates, however we prefer to rely on the general SED, which is better fit by L1 templates, than on a single feature that can be uncertain bearing in mind the poorly understood effects of low metallicity.

We also note that the water vapour absorption band at ∼ 1.5 μm, in the blue part of the *H*-band is more intense in this object than in early L dwarfs and more resembles mid/late L dwarfs. This is not an instrumental effect since it does not appear in the M8.5 object, but it may be due to a larger contamination by the primary at blue wavelengths than at red wavelengths. We therefore cannot, with confidence, assign this feature as unusual for this object. In summary, we estimate that HD 221356 D is a slightly blue early L dwarf with a spectral type of L0–L2.

3 PHYSICAL PROPERTIES OF HD 221356D

Assuming a distance of 26.12±0.37 pc to the system, we calculated the absolute magnitudes of individual components and constructed the $(M_I,\ I-J)$ and $(M_J,\ J-K_s)$ colour-magnitude diagrams, shown in Fig. 4. All four objects clearly follow a well defined photometric sequence, with the new companion located between the known B and C components. All the colours and magnitudes of the new object are in good agreement with its physical membership to the HD 221356 system. To better illustrate the position of the three low mass companions, we added in both panels of Fig. 4 the Pleiades low-mass stars and brown dwarfs (at d = 120 pc) from Bihain et al. (2010), M and L dwarfs from Liebert & Gizis (2006) with available parallaxes and the field M dwarfs from Leggett et al. (2000). The Pleiades cluster offers a homogeneous collection of objects with similar age and metallicity. The right panel also includes L and T dwarfs from Vrba & et al. (2004), Kirkpatrick et al. (2011), and 12 subdwarfs with spectral types from M7 to L7 with measured parallaxes (Faherty & et al. 2012). In the $(M_I,\ I-J)$ diagram we have also plotted the 5 Gyr isochrones of the NextGen models for solar and low metallicity ($[\mathrm{M/H}] = -0.5$) (Baraffe et al. 1998) and of the DUSTY model for solar metallicity (Chabrier et al. 2000).

We have depicted a veriety of objects with similar spectral types, that span from young ages (∼120 Myr) and solar composition, to old stars with solar metallicities and field subdwarfs with metal-poor abundances ([Fe/H]∼ −0.5, Lépine et al. 2007). The low-mass components of the HD 221356 system have slightly bluer colours than typical field stars, placing them on the blue edge of the photometric sequence defined by late M and L dwarfs. However their colours are redder than known field subdwarfs, implying an intermediate metallicity, being thus in good agreement with the metallicity determination of the primary. The $J-K_s$ and $I-J$ colours of the new companion, which are 1.01 ± 0.06 and 2.94 ± 0.14 mag respectively, correspond to the typical values of M7–M9 field dwarfs(Leggett & et al. 2002; Kirkpatrick & McCarthy 1994). These photometric colours suggest an earlier spectral type than that determined in the spectroscopic analysis. We attribute this difference to the sub-solar metallicity of the system, which affects the spectral energy distribution. In particular, the flux suppression in the K_s-band was already recognized in a group of L dwarfs, as a low metallicity feature (Kirkpatrick & et al. 2010; West et al. 2011). Because of that, the spectral classification of the wide binary components of the HD 221356 system, which is based on photometry, may be uncertain.

The luminosities of the B, C and D components were derived from their JHK_s-band magnitudes, using the trigonometric distance of the primary, bolometric corrections from Golimowski & et al. (2004) and spectral type-colour relations from Vrba & et al. (2004).

Table 3. Photometric data for the components of the multiple system HD 221356.

Component	I (mag)	Y (mag)	J (mag)	H (mag)	K_s (mag)
A	5.953±0.018	...	5.488±0.019	5.264±0.038	5.150±0.017
BC	15.536±0.027	13.695±0.025	12.852±0.010	12.261±0.026	11.946±0.026
B	15.568±0.018	...	12.933±0.011	12.353±0.026	12.055±0.028
C	19.363±0.039	...	15.713±0.042	14.993±0.061	14.495±0.114
D	16.70±0.10	14.933±0.059	13.763±0.038	13.209±0.026	12.755±0.025

Notes: I-band mag of A is from the FastCam, JHK_s mag are from 2MASS. I mag of the BC is from Gizis et al. (2003), JHK_s mags are from VHS and were decomposed using the flux ratios derived by Close et al. (2002). I mag of D is from IAC80 measurement, JHK_s mags are from our photometry on VHS images.

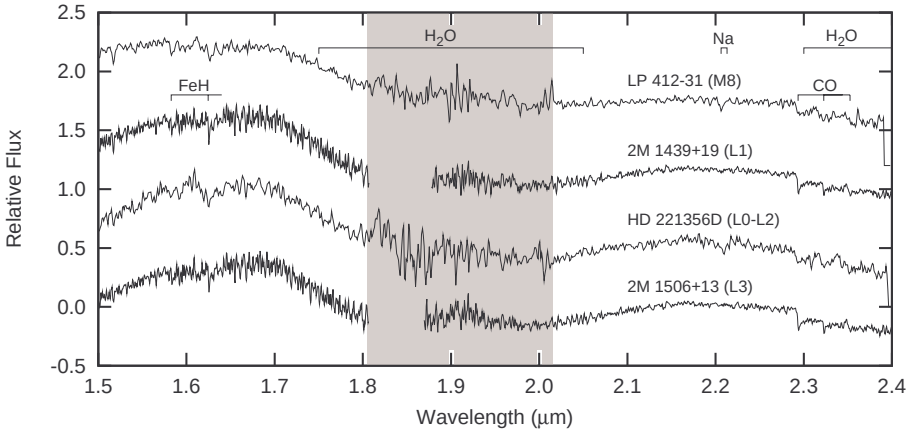

Figure 3. Near-infrared H- and K_s- band spectra of the new companion compared with the M8 standard LP 412-31 (Kirkpatrick et al. 1995), observed with the same instrumentation, and the L1 (2MASS J14392836+1929149) and L3 templates (2MASS J15065441+1321060) taken from the IRTF library (Cushing et al. 2005). Spectra were normalised at 1.7 microns and offsets have been added for clarity. The grey area indicates the region of high telluric absorption. The most prominent molecular and atomic features are indicated.

Table 4. Physical properties of low mass companions in HD 221356 system.

Comp.	SpType	log $L/L_\odot$	$T_{\rm eff}$ (K)	$M/M_\odot$
B	M8.0 ± 1.5	-3.28 ± 0.09	2351−2717	0.090 ± 0.008
C	L3.0 ± 1.5	-4.35 ± 0.09	1756−2141	$0.065^{+0.007}_{-0.016}$
D	L1.0 ± 1.0	-3.61 ± 0.10	2079−2304	0.079 ± 0.006

The effective temperature ranges were calculated adopting the temperature scale for high-gravity field dwarfs given by Golimowski & et al. (2004), assuming a spectral type range of L0–L2 for the new companion and M6.5–M9.5, L1.5–L4.5 for B and C, respectively. The resulting values are given in Table 4. The masses of the new companion and B and C components were estimated using the DUSTY model from the Lyon group (Chabrier et al. 2000), which is only available for solar metallicity. We adopted a wide range of ages, using the 1, 5 and 10 Gyr isochrones. Masses were derived from their luminosities by interpolating the mass-luminosity relations given in the models. The differences in mass calculated for different ages are lower than the errors in mass determination resulting from the uncertainties of luminosities. For the new companion we finally adopted a mass of $0.079\pm0.006M_\odot$, which is the average value obtained using JHK_s-band magnitudes, a spectral type range of L0−L2, and an age range of 1−10 Gyr. To take account of the differences in models for low metallicity stars, we have checked the mass of object D using the 5 Gyr NextGen model for $[M/H]=-0.5$ (Baraffe et al. 1998). We obtained a mass of 0.083 ± 0.002, which is slightly larger, but still within the uncertainties of that determined for solar metallicity models.

4 A BENCHMARK SUB-SOLAR METALLICITY MULTIPLE SYSTEM

The age of the primary star in the HD 221356 multiple system was estimated by Valenti & Fischer (2005) to be 2.5−7.9 Gyrs based on isochrone analysis. The lithium abundance of the primary star ($\log n(Li)=2.5$ in the usual scale of $\log n(H)=12$) is typical of late F-type stars in clusters with ages in the 2−8 Gyr range (Sestito & Randich 2005). The chromospheric activity of the star is also typical of a moderately old main sequence star (Valenti & Fischer 2005).

HD 221356 is a slightly metal-poor stellar system whose components have masses just above and below the hydrogen burning limit. For sub-solar metallicities the stellar–brown dwarf borderline is expected to be shifted to higher masses, e.g. to $\sim 0.079\,M_\odot$ at $[M/H]=-0.5$ ($0.072\,M_\odot$ at $[M/H]=0$) (Baraffe et al. 1998). In such a coeval, old system it becomes particularly interesting to investigate the lithium abundances of the very low mass components. While the M8 star (component B) and the L0−L2 (component D) should have fully burnt their original lithium, component C with 0.065 solar mass may have preserved some amount of the initial lithium content. Theoretical models for solar metallicity predict full lithium depletion for such a mass, however this may not be the case for sub-solar metallicity, since models also predict a less efficient

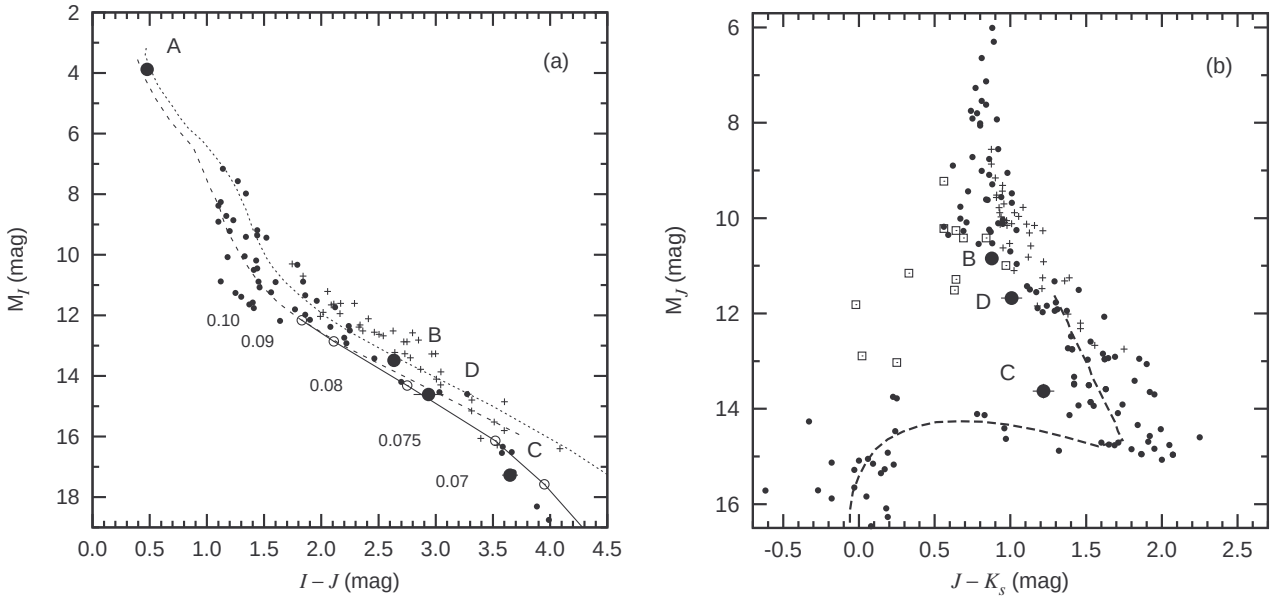

Figure 4. Left panel: M_I, $I-J$ colour-magnitude diagram of the HD 221356 system. The positions of the four components are marked with points and labelled with the corresponding letters. Pleiades low-mass stars and brown dwarfs (crosses) from Bihain et al. (2010), M and L dwarfs from Liebert & Gizis (2006) with available parallaxes and M dwarfs (dots) from Leggett et al. (2000) are also plotted. The 5 Gyr isochrones of the NextGen models for solar and low metallicity stars (Baraffe et al. 1998), represented by a dotted and dashed line, respectively, and of the DUSTY model for solar metallicity (Chabrier et al. 2000), shown as a solid line, are also included. The masses in solar mass units from the DUSTY model are also indicated and marked with open circles in the corresponding isochrone. Right panel: M_J, $J-K$ of BCD components of the HD 221356 system. We have also added L and T dwarfs from Vrba & et al. (2004) and Kirkpatrick et al. (2011) and 12 subdwarfs with measured parallaxes from Faherty & et al. (2012), depicted by squares. The mean L and T near-infrared photometric sequence from Vrba & et al. (2004) is represented by a dashed line.

depletion at low metallicities (Chabrier & Baraffe 1997). Observations of the Li abundance in the three low-mass components of this system will constrain both the evolutionary models and the age of the system.

Multi epoch measurements of the system will allow to detect the orbital motion of companion D. Although the estimated orbital period (assuming circular orbit) is of the order of 5500 years, the relative change of the position would be up to ~ 14 mas/yr, which is measurable using modern high spatial resolution imaging (e.g., adaptive optics, lucky imaging). The expected semi-amplitude of radial velocity variation of the primary induced by the presence of companion D will be of the order of 130 m/s (for 90^{o} inclination), however the orbital period is too long to allow a full determination of the three-dimensional orbit. Maximum annual variations of roughly 0.15 m/s are expected, which may be explored with the new generation of ultra high precision spectrographs (Wilken & et al. 2012).

5 CONCLUSIONS

Using the VHS and 2MASS surveys we have identified a new very low-mass companion (HD 221356 D) in the slightly metal-poor HD 221356 system, which thus becomes a quadruple. The new object is located at a projected distance of ~ 312 AU from the F8 primary. The four components of the system follow a well defined photometric sequence. From near-infrared spectroscopy we determined L0–L2 spectral type for the D companion. Based on evolutionary models its mass is estimated at 0.079 ± 0.006 $M_{\odot}$, and its effective temperature is in the range from 2100 to 2300 K. The $J-K_s$ and $I-J$ colours of the low-mass components are slightly bluer than field counterparts of the same spectral type. We interpret this as a result of the low metallicity of the system, which may become a reference for the spectral classification of metal poor M and L-type field objects. Since the distance and metallicity of the HD 221356 system are well known, the detailed study of its ultracool companions, which are located above and below the frontier between stars and brown dwarfs, can provide valuable constrains on evolutionary models and, in particular, shed light on the properties of objects on the transition from stellar to substellar regime.

Acknowledgements. Based on observations obtained as part of the VISTA Hemisphere Survey, ESO Program; 179.A-2010 (PI: McMahon). The VISTA Data Flow System pipeline processing and science archive are described in Irwin & et al. (2004) and Cross et al. (2009). This article is based on observations made with the TCS and IAC80 telescope operated on the island of Tenerife by the IAC in the Spanish Observatorio del Teide, and with the William Herschel Telescope operated on the island of La Palma by the Isaac Newton Group in the Spanish Observatorio del Roque de los Muchachos of the Instituto de Astrofísica de Canarias. This publication makes use of data products from the Two Micron All Sky Survey, which is a joint project of the University of Massachusetts and the Infrared Processing and Analysis Center/California Institute of Technology, funded by the National Aeronautics and Space Administration and the National Science Foundation. This research has benefitted from the SpeX Prism Spectral Libraries, maintained by Adam Burgasser at http://pono.ucsd.edu/∼adam/browndwarfs/spexprism. This research has been supported by the Spanish Ministry of Economics and Competitiveness under the projects AYA2010-21308-C3-02, AYA2010-21308-C03-03 and AYA2010-20535. V.J.S.B. and N. L. are partially supported by the Spanish Ramón y Cajal program.

REFERENCES

Allers K. N., et al. 2007, ApJ, 657, 511
Baraffe I., Chabrier G., Allard F., Hauschildt P. H., 1998, A&A, 337, 403
Bean J. L., Sneden C., Hauschildt P. H., Johns-Krull C. M., Benedict G. F., 2006, ApJ, 652, 1604
Bihain G., Rebolo R., Zapatero Osorio M. R., Béjar V. J. S., Caballero J. A., 2010, A&A, 519, A93
Bonfils X., Delfosse X., Udry S., Santos N. C., Forveille T., Ségransan D., 2005, A&A, 442, 635
Burgasser A. J., Reid I. N., Siegler N., Close L., Allen P., Lowrance P., Gizis J., 2007, Protostars and Planets V, pp 427–441
Burrows A., et al. 1997, ApJ, 491, 856
Burrows A., Hubbard W. B., Lunine J. I., Liebert J., 2001, Reviews of Modern Physics, 73, 719
Caballero J. A., 2007, ApJ, 667, 520
Chabrier G., Baraffe I., 1997, A&A, 327, 1039
Chabrier G., Baraffe I., Allard F., Hauschildt P., 2000, ApJ, 542, 464
Close L. M., Siegler N., Potter D., Brandner W., Liebert J., 2002, ApJ, 567, L53
Costado M. T., Béjar V. J. S., Caballero J. A., Rebolo R., Acosta-Pulido J., Manchado A., 2005, A&A, 443, 1021
Cross N. J. G., Collins R. S., Hambly N. C., Blake R. P., Read M. A., Sutorius E. T. W., Mann R. G., Williams P. M., 2009, MNRAS, 399, 1730
Cushing M. C., Rayner J. T., Vacca W. D., 2005, ApJ, 623, 1115
Dupuy T. J., Liu M. C., Bowler B. P., Cushing M. C., Helling C., Witte S., Hauschildt P., 2010, ApJ, 721, 1725
Emerson J., McPherson A., Sutherland W., 2006, The Messenger, 126, 41
Epchtein N., et al. 1999, A%A, 349, 236
Faherty J. K., Burgasser A. J., West A. A., Bochanski J. J., Cruz K. L., Shara M. M., Walter F. M., 2010, AJ, 139, 176
Faherty J. K., et al. 2012, ApJ, 752, 56
Gizis J. E., Monet D. G., Reid I. N., Kirkpatrick J. D., Liebert J., Williams R. J., 2000, AJ, 120, 1085
Gizis J. E., Reid I. N., Knapp G. R., Liebert J., Kirkpatrick J. D., Koerner D. W., Burgasser A. J., 2003, AJ, 125, 3302
Golimowski D. A., et al. 2004, AJ, 127, 3516
Irwin M. J., et al. 2004, in Quinn P. J., Bridger A., eds, Society of Photo-Optical Instrumentation Engineers (SPIE) Conference Series Vol. 5493 of Society of Photo-Optical Instrumentation Engineers (SPIE) Conference Series, VISTA data flow system: pipeline processing for WFCAM and VISTA. pp 411–422
Kirkpatrick J. D., Cushing M. C., Gelino C. R., 2011, ApJS, 197, 19
Kirkpatrick J. D., et al. 2010, ApJS, 190, 100
Kirkpatrick J. D., Henry T. J., Simons D. A., 1995, AJ, 109, 797
Kirkpatrick J. D., McCarthy Jr. D. W., 1994, AJ, 107, 333
Kraus A. L., Hillenbrand L. A., 2007, ApJ, 662, 413
Lafrenière D., et al. 2007, ApJ, 670, 1367
Landolt A. U., 1992, AJ, 104, 340
Leggett S. K., Allard F., Dahn C., Hauschildt P. H., Kerr T. H., Rayner J., 2000, ApJ, 535, 965
Leggett S. K., et al. 2002, ApJ, 564, 452
Lépine S., Rich R. M., Shara M. M., 2007, ApJ, 669, 1235
Lewis J. R., Irwin M., Bunclark P., 2010, in Y. Mizumoto, K.-I. Morita, & M. Ohishi ed., Astronomical Data Analysis Software and Systems XIX Vol. 434 of Astronomical Society of the Pacific Conference Series, Pipeline Processing for VISTA. p. 91
Liebert J., Gizis J. E., 2006, PASP, 118, 659
McCarthy C., Zuckerman B., 2004, AJ, 127, 2871
Oscoz A., et al. 2008, in Society of Photo-Optical Instrumentation Engineers (SPIE) Conference Series Vol. 7014 of Society of Photo-Optical Instrumentation Engineers (SPIE) Conference Series, FastCam: a new lucky imaging instrument for medium-sized telescopes
Pinfield D. J., et al. 2012, MNRAS, 422, 1922
Pinfield D. J., Jones H. R. A., Lucas P. W., Kendall T. R., Folkes S. L., Day-Jones A. C., Chappelle R. J., Steele I. A., 2006, MNRAS, 368, 1281
Sestito P., Randich S., 2005, A&A, 442, 615
Skrutskie M. F., et al. 2006, AJ, 131, 1163
Slesnick C. L., Hillenbrand L. A., Carpenter J. M., 2004, ApJ, 610, 1045
Testi L., et al. 2001, ApJL, 552, L147
Valenti J. A., Fischer D. A., 2005, ApJS, 159, 141
van Leeuwen F., 2007, A&A, 474, 653
Vrba F. J., et al. 2004, AJ, 127, 2948
West A. A., Bochanski J. J., Bowler B. P., Dotter A., Johnson J. A., Lépine S., Rojas-Ayala B., Schweitzer A., 2011, in Johns-Krull C., Browning M. K., West A. A., eds, 16th Cambridge Workshop on Cool Stars, Stellar Systems, and the Sun Vol. 448 of Astronomical Society of the Pacific Conference Series. p. 531
Wilken T., et al. 2012, Nature, 485, 611
Zhang Z. H., et al. 2010, MNRAS, 404, 1817